Invited Paper

Shape Control of Composite Material Plates Using Piezoelectric Actuators

Brij N. Agrawal* and M. Adnan Elshafei+

Spacecraft Research and Design Center (SRDC)
Department of Aeronautics and Astronautics
The Naval Postgraduate School
Monterey, CA 93940, USA

ABSTRACT

This paper concerns the shape control of composite material plates using piezoelectric actuators. A finite element formulation is developed for modeling a laminated composite plate that has piezoelectric actuators and sensors. To improve the accuracy of the prediction of the plate deformation, a simple higher-order deformation theory is used. The electrical potential is treated as a generalized coordinate, allowing it to vary over the element. For the shape control, an optimization algorithm, based on finite element techniques, is developed to determine optimal actuator voltages to minimize the surface error between the desired shape and actual deformed shape. The error function for a plate element is determined by calculating the mean square of the surface error over the surface, instead of determining it only at the node points of the element. Based on these techniques, Matlab codes were developed. Analyses were performed to determine optimum actuator voltages. The analytical results demonstrate the feasibility of using piezoelectric actuators for the active shape control of spacecraft reflectors.

Keywords: composite material plates, piezoelectric actuators, shape control, intelligent structure, finite element

1. INTRODUCTION

In general, smart structures are the elements of system that are able to sense the state of structure and change it as the system demands. There have been a number of recent studies[1] on the use of smart structures for vibration control, shape control, and noise reduction. Some of these applications are for spacecraft antennas to compensate for surface errors introduced by manufacturing errors, thermal distortion in orbit, moisture, material degradation, and creep. They can be also used to change antenna beam shape in-orbit as the demand for antenna coverage changes. They may be used for submarine and helicopter shape control. An aeroelastic application to aircraft structures is quasi-static control of camber, dynamic control, and flutter suppression. Smart structures can be used in acoustic control by developing adaptive structures in which the structural response can be modified with varying input disturbances. A number of materials are available which may be used as sensor or actuator elements of smart structures. These material include piezoelectric polymers and ceramics, shape memory alloys, and optical fibers. While substantial research effort has been devoted to the use of smart structures for active vibration suppression, considerable less attention has been focused on the use of smart structures for shape control.

Active vibration and shape control using smart structures is an active area of research at the Spacecraft Research and Design Center at the Naval Postgraduate School. This paper presents the recent results on the shape control of composite plates, a common structural element for aerospace structures, using piezoelectric actuators. Although piezoelectric actuators are limited to the production of relatively small deformation, their application may be more than adequate for certain applications, such as compensating for thermal distortion and manufacturing errors in precision spacecraft antennas.

The research work presented in this paper is performed in three parts. First, a finite element model of graphite/epoxy laminate plate is developed using a simple higher-order shear deformation theory. Generally, classical plate theory has been used in which it is assumed that normal to the mid-plane before deformation remains straight and normal to

* Professor and Director of SRDC
+ Lt. Col. Egyptian Air Force

SPIE Vol. 3241 • 0277-786X/97/$10.00

the mid-plane after deformation. This theory under predicts deflection and over predicts natural frequencies and buckling loads. These errors are due to the neglect of transverse shear strains in the classical theory. Several higher-order laminated plate theories have been proposed. However, a compromise is required between accuracy and ease of analysis. A simple higher-order theory described by Reddy[2] is such a theory, as it accounts not only for transverse shear strain but also its parabolic variation across the thickness of the plate. This theory is used in this paper in the development of the finite element model. In the second part, a finite element model is expanded to include distributed piezoelectric actuators and sensors. The electric potential is treated as a generalized electric coordinate, like generalized displacement coordinate. This approach allows the variation of electric potential across the surface of the element. In the third part, an optimization algorithm is developed to determine optimal actuator voltages to minimize the error between the desired shape and the actual shape. A few studies have been done on the shape control. Ghosh[3] showed a model for plate shape control by using PZT, Agrawal[4] developed a mathematical model for deflection using a finite difference technique and estimated the optimal actuation voltages. Koconis[5] presented an analytical method to determine the voltages needed to achieve a specified desired shape with minimum error between the actual shape and the desired shape. The error function is defined as the mean square of the error between the points in the actual deformed surface and in the desired surface integrated over the surface of the element. Matlab optimization functions are used for minimizing the error function and determining optimum actuator voltages.

2. FINITE ELEMENT MODEL

The finite element model of the plate element is based on the following displacement field

$$U(x,y,z) = U_0 + z\left[\phi_{x0} - \frac{4}{3}\left(\frac{z}{t}\right)^2\left(\phi_{x0}+\partial w/\partial x\right)\right] \tag{1}$$

$$V(x,y,z) = V_0 + z\left[\phi_{y0} - \frac{4}{3}\left(\frac{z}{t}\right)^2\left(\phi_{y0}+\partial w/\partial y\right)\right]$$

$$W(x,y,z) = W_0$$

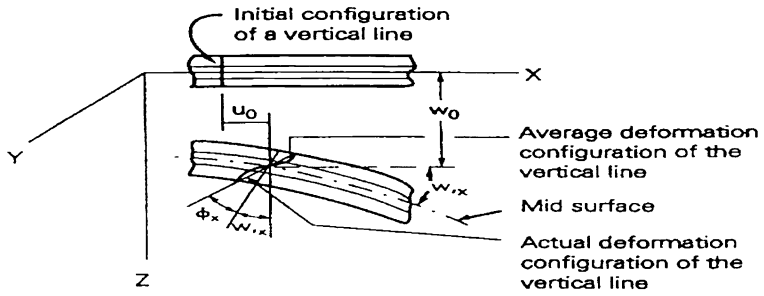

Figure 1. Deformation of the plate element

where U_0, V_0, and W_0 , as shown in Fig. 1, are the displacement of a point on the mid-plane in X, Y, and Z axes, respectively; ϕ_x, ϕ_y are the average rotations about the Y and X axes, respectively, of the normal to the mid-plane of the undeformed plate; z is the distance of a point from the mid-plane along the Z axis, and t is the thickness of the plate.

The strain at any point is given by

$$\{\varepsilon\} = \begin{Bmatrix} \varepsilon_x^0 \\ \varepsilon_y^0 \\ \varepsilon_{xy}^0 \\ \varepsilon_{xz}^0 \\ \varepsilon_{yz}^0 \end{Bmatrix} + z\begin{Bmatrix} K_x^1 \\ K_y^1 \\ K_{xy}^1 \\ 0 \\ 0 \end{Bmatrix} + z^2\begin{Bmatrix} 0 \\ 0 \\ 0 \\ K_{xz}^2 \\ K_{yz}^2 \end{Bmatrix} + z^3\begin{Bmatrix} K_x^3 \\ K_y^3 \\ K_{xy}^3 \\ 0 \\ 0 \end{Bmatrix} \tag{2}$$

where;

$$\varepsilon_x^0 = U_{0,x};$$
$$\varepsilon_y^0 = V_{0,y};$$
$$\varepsilon_{xy}^0 = U_{0,y} + V_{0,x};$$
$$\varepsilon_{xz}^0 = \phi_{x0} + W_{0,x};$$
$$\varepsilon_{yz}^0 = \phi_{y0} + W_{0,y};$$
$$K_x^1 = \phi_{x0,x};$$
$$K_y^1 = \phi_{y0,y};$$
$$K_{xy}^1 = \phi_{x0,y} + \phi_{y0,x};$$
$$K_{xz}^2 = -4(\partial w/\partial x + \phi_{x0})/t^2;$$
$$K_{yz}^2 = -4(\partial w/\partial y + \phi_{y0})/t^2;$$
$$K_x^3 = -4(\partial^2 w/\partial x^2 + \phi_{xo,x})/(3t^2);$$
$$K_y^3 = -4(\partial^2 w/\partial y^2 + \phi_{y0,y})/(3t^2);$$

and

$$K_{xy}^3 = -4(2\partial^2 w/\partial x\partial y + \phi_{x0,y} + \phi_{y0,x})/3t^2); \tag{3}$$

The strain terms include linear strain, curvatures, twists and higher-order curvatures.

A composite plate with distributed piezoelectric actuators and sensors is shown in Fig. 2. A typical elastic/piezoelectric structure is composed of a aluminum or graphite/epoxy structure with bonded or embedded piezoelectric sensors and actuators.

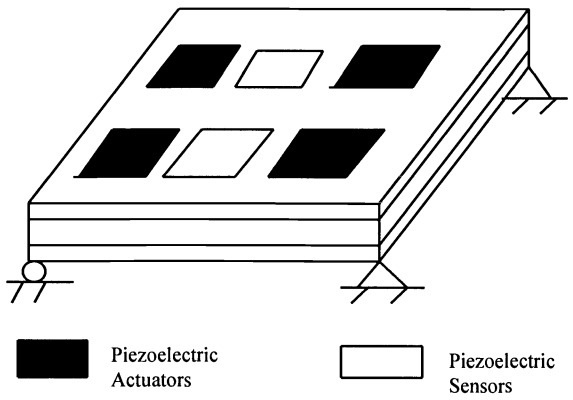

Figure 2. Composite Plate with distributed piezoelectric sensors and actuators

The linear piezoelectric constitutive equations coupling the elastic field and electric field are expressed as:

$$\{D\} = [e]^T\{\varepsilon\} + [\varepsilon^s]\{E\} \tag{4}$$

$$\{\sigma\} = [c]\{\varepsilon\} - [e]\{E\} \tag{5}$$

where D is electric displacement (C/m^2), e is dielectric permitivity matrix (C/m^2), ε is strain vector, ε^s is dielectric matrix at constant mechanical strain (F/m), E is electric vector (V/m), σ is stress vector (N/m^2), c is elasticity matrix for a constant electric field (N/m^2).

It is assumed that the principal material coordinates coincide with the coordinates of the element. For the material having orthohomic mm2 symmetry, including piezoelectric effects, and plane stress conditions; the constitutive relations are given by

$$\begin{Bmatrix} D_x \\ D_y \\ D_z \end{Bmatrix} = \begin{bmatrix} 0 & 0 & 0 & \bar{e}_{15} & 0 \\ 0 & 0 & \bar{e}_{24} & 0 & 0 \\ \bar{e}_{31} & \bar{e}_{32} & 0 & 0 & 0 \end{bmatrix} \begin{Bmatrix} \varepsilon_x \\ \varepsilon_y \\ \varepsilon_{xy} \\ \varepsilon_{xz} \\ \varepsilon_{yz} \end{Bmatrix} + \begin{bmatrix} \bar{\varepsilon}^s_{11} & 0 & 0 \\ 0 & \bar{\varepsilon}^s_{22} & 0 \\ 0 & 0 & \bar{\varepsilon}^s_{33} \end{bmatrix} \begin{Bmatrix} E_x \\ E_y \\ E_z \end{Bmatrix} \tag{6}$$

$$\begin{Bmatrix} \sigma_x \\ \sigma_y \\ \sigma_{xy} \\ \sigma_{xz} \\ \sigma_{yz} \end{Bmatrix} = \begin{bmatrix} \bar{c}_{11} & \bar{c}_{12} & 0 & 0 & 0 \\ \bar{c}_{21} & \bar{c}_{22} & 0 & 0 & 0 \\ 0 & 0 & \bar{c}_{44} & 0 & 0 \\ 0 & 0 & 0 & \bar{c}_{55} & 0 \\ 0 & 0 & 0 & 0 & \bar{c}_{66} \end{bmatrix} \begin{Bmatrix} \varepsilon_x \\ \varepsilon_y \\ \varepsilon_{xy} \\ \varepsilon_{xz} \\ \varepsilon_{yz} \end{Bmatrix} - \begin{bmatrix} 0 & 0 & \bar{e}_{31} \\ 0 & 0 & \bar{e}_{32} \\ 0 & \bar{e}_{24} & 0 \\ \bar{e}_{15} & 0 & 0 \\ 0 & 0 & 0 \end{bmatrix} \begin{Bmatrix} E_x \\ E_y \\ E_z \end{Bmatrix} \tag{7}$$

Hamilton's Principle is used to determine the equations of motion. The Lagrangian $\Im$ of a piezoelectric body is defined in terms of kinetic energy and potential energy (including strain and electrical energies). The Lagrangian for a piezoelectric body is

$$\Im = \int_V \left[\frac{1}{2}\rho\{\dot{q}\}^T\{\dot{q}\} - \frac{1}{2}\left(\{\varepsilon\}^T\{\sigma\} - \{E\}^T\{D\}\right)\right] dV \tag{8}$$

where $\dot{q}$ is the velocity and V is piezoelectric volume. For non-piezoelectric elements, the last term in Lagrangian due to electrical energy will be absent. The virtual work done by the external force and the surface charge density, μ ,applied to the piezoelectric body is

$$\delta W = \int_{s1} \{\delta q\}^T \{P_s\} ds_1 - \int_{s2} \delta\Phi\mu ds_2 \tag{9}$$

where s_1 and s_2 are the surfaces at which the mechanical loads are applied, respectively, P_s is a surface load and Φ is the electric potential.

Hamilton's principle is

$$\int_{t1}^{2} \delta(\Im + W) dt = 0, \tag{10}$$

where t_1 to t_2 is the interval, and all variations must vanish at $t = t_1$ and $t = t_2$.

Substituting Eqs (8) and (9) into Eq. (10), we get

$$\int_v \left[\rho\{\partial q\}^T\{\ddot{q}\} + \{\delta\varepsilon\}^T[c]\{\varepsilon\} - \{\delta\varepsilon\}^T[e]\{E\} - \{\delta E\}^T[e]^T\{\varepsilon\} - \{\delta E\}^T[\varepsilon^s]\{E\}\right]dv$$
$$- \int_{s_1}\{\delta q\}^T\{P_s\}ds_1 + \int_{s_2}\delta\Phi\mu ds_2 = 0 \tag{11}$$

To generate the electro-elastic matrix relations, it was assumed that the surface of the piezoelectric layers which are in contact with the laminated substructures are suitably grounded. Also, since the thickness of the piezoelectric layers is very small, it is reasonable to assume that the electric potential functions, which yield zero potential at the interface between the actuator and laminated substructure and provide a linear variation across the thickness of the sensor or actuator layer,are as follows:

$$\Phi^L(x,y,z) = (z - h_{Lp})\Phi_0^L(x,y) \tag{12}$$

where Φ_0^L can be treated as the generalized electric coordinate similar to the generalized displacement coordinate at the mid-plane of the plate element.

2.1 Finite Element Formulation

The objective is to define the degrees of freedom U_o, V_o, ϕ_{xo}, ϕ_{yo}, W_o, W_x,W_y, and Φ in the plate in terms of nodal displacements, rotations, and electric coordinates by using a bilinear, isoparametric, rectangular element with four nodes. Each node of the element has eight degrees of freedom. Similar interpolation functions are used for displacements U_0 and V_0, rotations ϕ_{x0} and ϕ_{y0}, and electrical coordinate Φ_0^L .They are defined by

$$p = \sum_{i=1}^{4} N_i p_i \tag{13}$$

where p is the value of the variable at any point in the element, p_i is its value at node point and N_i is the interpolation function, which in the natural coordinate system (ξ , η) is

$$N_i = 1/4(1+\xi\xi_i)(1+\eta\eta_i) \tag{14}$$

where ξ and η are the local coordinates of the point, and ξ_i = -1,1,1,-1 and η_i = -1,-1,1,1 for i = 1,...,4, as shown in Fig.3.

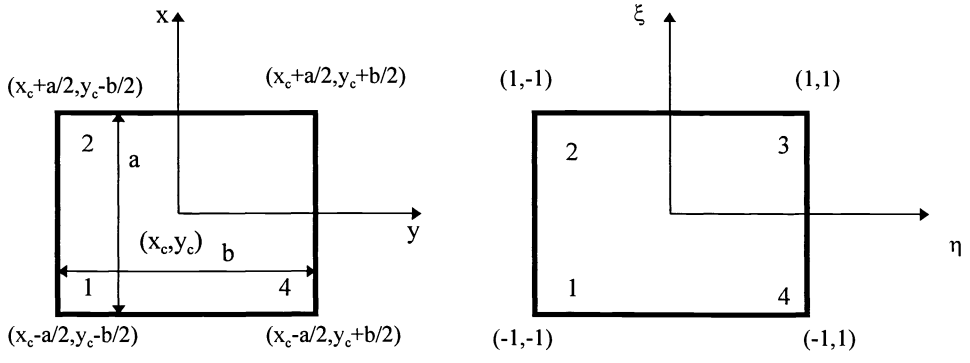

Figure 3 Actual and Master Element

The transverse displacement is interpolated using a non-conforming shape function which can be given by:

$$w(x,y) = \begin{bmatrix} f_1 & g_1 & h_1 & f_2 & g_2 & h_2 & f_3 & g_3 & h_3 & f_4 & g_4 & h_4 \end{bmatrix} \begin{bmatrix} w_{01} \\ w_{,x1} \\ w_{,y1} \\ w_{02} \\ \cdot \\ \cdot \\ \cdot \\ w_{,x4} \\ w_{,y4} \end{bmatrix} \tag{15}$$

where for $i = 1,\ldots,4$

$$\begin{aligned} f_i &= \frac{1}{8}(1+\xi\xi_i)(1+\eta\eta_i)(2+\xi\xi_i+\eta\eta_i-\eta^2-\xi^2) \\ g_i &= (a/16)\xi_i(1+\xi\xi_i)^2(1+\eta\eta_i)(\xi\xi_i-1) \\ h_i &= (b/16)\eta_i(1+\eta\eta_i)^2(1+\xi\xi_i)(\eta\eta_i-1) \end{aligned} \tag{16}$$

where

$$\xi = 2(x-x_c)/a, \quad \eta = 2(y-y_c)/b, \tag{17}$$

The nodal displacement vector $\{q_1\}$ at the first node point on the plate element is

$$\{q_1\} = \begin{bmatrix} U_{01} & V_{01} & \phi_{x01} & \phi_{y01} & w_{01} & w_{,x1} & w_{,y1} \end{bmatrix}^T \tag{18}$$

and the element displacement vector $\{q_e\}$ is

$$\{q_e\} = \begin{bmatrix} q_1 & q_2 & q_3 & q_4 \end{bmatrix}^T \tag{19}$$

The generalized displacement vector at a point is

$$\{q\} = \begin{bmatrix} U_0 & V_0 & \phi_{x0} & \phi_{y0} & w_0 & w_{,x0} & w_{,y0} \end{bmatrix}^T \tag{20}$$

The generalized electric coordinate at the ith node of element is Φ_{0i}^e and the element nodal generalized electric coordinate vector is given by

$$\{\Phi_0^e\} = \begin{bmatrix} \Phi_{01}^e & \Phi_{02}^e & \Phi_{03}^e & \Phi_{04}^e \end{bmatrix}^T \tag{21}$$

Substituting displacement and electric coordinates in terms of nodal coordinates, the equations of motion for the element, using Eq. (11), becomes

$$\begin{aligned} [M_e]\{\ddot{q}_e\} + [k_{qq}]\{q_e\} - [k_{q\Phi}]\{\Phi_0^e\} &= \{P_M\} \\ [k_{\Phi q}]\{q_e\} + [k_{\Phi\Phi}]\{\Phi_0^e\} &= \{g\} \end{aligned} \tag{22}$$

It should be noted that the mechanical equation is coupled with the electrical equation and $\{P_M\}$ is the mechanical excitation and $\{g\}$ is the electrical excitation. $[M_e]$ is element mass matrix, [k] are stiffness and interaction matrices between actuator potential and displacement. Assembling the element equations and using a constraint equation, the equation of motion of the structure system is obtained.

3. SHAPE CONTROL

The objective is to determine optimum actuator voltages for given actuator locations to minimize the error between the desired shape and achieved shape. The analysis is based on the small deformation theory. Figure 4 shows the original surface, deformed surface with the application of actuators, and desired surface.

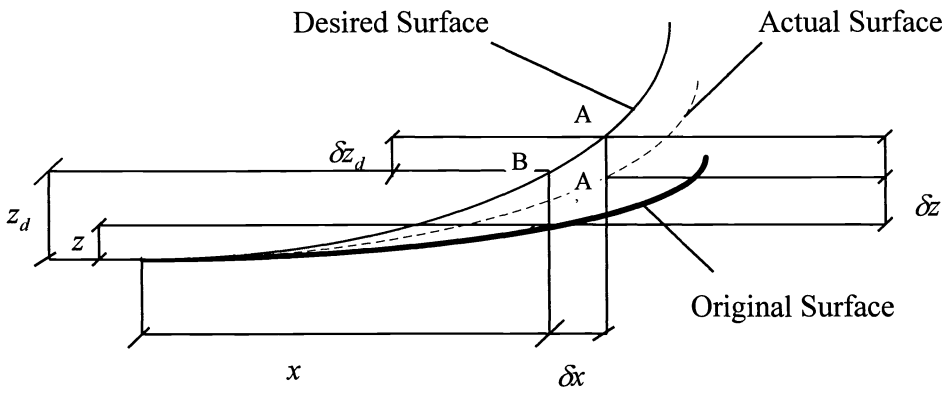

Figure 4 Original Surface, Actual Surface, and Desired Surface in the x-z plane

The error function takes the form:

$$\Lambda_e^i = \int_{\Omega_e} \Delta^2 dxdy \tag{23}$$

where Λ_e^i is the error function of the ith element, Ω_e is the element domain, Δ represents the difference between the z-coordinate on the reference surface of the desired shape and the z-coordinate of a corresponding point on the actual deformed surface. The error function of the total surface will be the sum of the error function of each element and is given by

$$\Lambda = \sum_{i=1}^{n} \Lambda_e^i \tag{24}$$

From Figure 4, the distance Δ is defined as:

$$\Delta = (z_0 + \delta z_0) - (z_{des} + \delta z_{des}) \tag{25}$$

To evaluate each term in this equation, we consider a nodal point A on the original reference surface at (x_0, y_0). Thus z_0 is the z coordinate of the point A on the original reference surface, δz_0 is the difference between the z-coordinate of point A on the original surface and the z coordinate of the corresponding point A' in the actual surface, which can be expressed as:

$$\delta z_0 = \left(\frac{\partial z_0}{\partial x} u + \frac{\partial z_0}{\partial y} v + w \right)_A \tag{26}$$

where u, v, and w are the displacement of the node A and z_{des} is the z-coordinate of point B on the desired reference surface at (x_0, y_0).

The point on the desired reference surface corresponding to point A' on the actual reference surface is point A" located at $(x_0 + \delta x_0, y_0 + \delta y_0)$. δz_{des} is the difference between z-coordinates of point A" and B. It can be approximated by the first two terms of a Taylor series expansion.

$$\delta z_{des} = \left(\frac{\partial z_{des}}{\partial x} \right)_B \delta x_0 + \left(\frac{\partial z_{des}}{\partial y} \right)_B \delta y_0 \tag{27}$$

The distances δx_0 and δy_0 are the changes in the x and y coordinates between A" and B and are given by

$$\delta x_0 = \left(u - w \frac{\partial z_0}{\partial x} \right)_A, \qquad \delta y_0 = \left(v - w \frac{\partial z_0}{\partial y} \right)_A \tag{28}$$

The following parameters are introduced which depend on the geometry of the original and desired surface,

$$\eta_1 = 1 + \left(\frac{\partial z_{des}}{\partial x} \right)_B \left(\frac{\partial z_0}{\partial x} \right)_A + \left(\frac{\partial z_{des}}{\partial y} \right)_B \left(\frac{\partial z_0}{\partial y} \right)_A \tag{29}$$

$$\eta_2 = \left(\frac{\partial z_0}{\partial x} \right)_A - \left(\frac{\partial z_{des}}{\partial x} \right)_B, \ldots\ldots \eta_3 = \left(\frac{\partial z_0}{\partial y} \right)_A - \left(\frac{\partial z_{des}}{\partial y} \right)_B$$

By using these parameters, the objective function will take the form:

$$\Lambda_e^i = \int_{\Omega_e} \left[(z_0 - z_{des}) + \eta_1 w + \eta_2 u + \eta_3 v \right]^2 dxdy \tag{30}$$

Similar to the previous section, we use finite elements, representing displacements in terms of nodal coordinates. The displacements at the nodal points can be expressed in terms of actuator voltages from Eq. (22). Using these transformations, the error function for one element in master element coordinates is written as:

$$\Lambda_e^i = \int_{-1}^{+1} \int_{-1}^{+1} \left[\left(z_0(\xi,\eta) - z_{des}(\xi,\eta) \right) + \eta_1(\xi,\eta) \tilde{w}(V) + \eta_2(\xi,\eta) \tilde{u}(V) + \eta_3(\xi,\eta) \tilde{v}(V) \right]^2 |J| d\xi d\eta \tag{31}$$

where ξ and η are the coordinates of the master element and $|J|$ is determinant of the Jacobian matrix of transformation.

The structure objective function is defined as the summation of the error function for each element as follows:

$$\Lambda = \sum_{i=1}^{n} \Lambda_e^i \tag{32}$$

subjected to constraint

Lower limit $\leq$ V $\leq$ Upper limit

where *n* is the number of elements and V is actuator electric potential.

4. OPTIMIZATION

Matlab optimization functions f-min and f-mins are used to find optimum actuator voltage to minimize the objective error function. The f-min function is used to minimize a function of one variable on a fixed interval. The problem is mathematically stated as:

$$\underset{x}{\text{minimize}}\ f(x) \qquad \text{subjected to: } x_1 \le x \le x_2 \tag{33}$$

where f(x) and x are scalars. The f-min function is used to optimize the objective function when the same voltage is applied to all actuators. The function permits putting a constraint on the maximum value of the actuator voltage.

The function f-mins is used to find the minimum of a scalar function of several variables and is mathematically stated as

$$\underset{x}{\text{minimize}}\ f(x) \tag{34}$$

where x is a vector and f is a scalar function. This optimization function does not provide constraint on x and is generally referred to as unconstrained nonlinear optimization. The function f-mins is used when different voltages are applied to the piezoelectric actuators (V is a vector). In this case we can not impose a constraint on the maximum value of the voltages. *f*-mins uses the simplex search algorithm of Nelder and Mead.

5. NUMERICAL ANALYSIS

Based on the techniques discussed in the previous sections, two Matlab codes were developed. The first code COMPZ is a finite element code to solve a laminated plate with piezoelectric actuators and subjected to mechanical and electrical loads. The second code OPTSHP determines change in the shape of the plate due to the application of actuator voltages and computes optimum actuator voltages to minimize the objective function.

To validate the code COMPZ, the results from this code for a composite plate with piezoelectric actuators were compared with the analytical results from Ref. 6 and finite element results from Ref. 7. The example used is a square plate consisting of a three-layered cross-ply laminated plate with the thickness 3 mm. Piezoelectric PVDF layer of 40μm was used and it covered the whole surface.

E_{11}= 172.4 GPa (25×10^6 psi)
$G_{12}=G_{13}$=3.45 GPa (0.5×10^6 psi);
$\nu_{12}=\nu_{13}$=0.25

E_{22}=6.9 GPa (10^6 psi);
G_{23}=1.38 GPa (0.2×10^6);

The piezoelectric PVDF layers properties are :

Dielectric permittivity
e_{31} = 0.0460 C/m^2
e_{32} = 0.0460 C/m^2
e_{33} = 0.0000 C/m^2

Dielectricity
$\varepsilon_{11}^s = 0.1062 \times 10^{-9}$ F/m
$\varepsilon_{22}^s = 0.1062 \times 10^{-9}$ F/m
$\varepsilon_{33}^s = 0.1062 \times 10^{-9}$ F/m

Poisson ratio $\nu = 0.29$
Mass density $\rho = 0.1800 \times 10^4$ kg/m^3
Modulus of elasticity $E=2 \times 10^{\wedge 4}$ N/m^2

The mechanical loading and the electrical potential distribution is described by:

$$q = q_0 \sin(\pi x / a)\sin(\pi y / b)$$

and

$$\Phi(x, y, h_{Op}) = V \sin(\pi x / a)\sin(\pi y / b);$$

where q_0 is the intensity of load per unit area (N/m^2), V is the amplitude of Φ in volts, and h_{op} is the height of piezoceramic outer layer. The deflection is normalized as :

$$\overline{w} = \frac{100 E_T}{q_0 \lambda h} w$$

where E_T is the transverse Young's modulus of the graphite/epoxy layers, λ is the span to the thickness ratio, and h is the structure thickness

Figure 5 shows the bending deflection at the center verses length to thickness ratio for the plate subjected to a double sinusoidal mechanical load. Figure 6 shows the bending deflection at the center verses length to thickness ratio for the plate subjected to a double sinusoidal distribution for both mechanical and electrical loads. The results generated by using COMPZ are compared with analytical results from Ref. 6 and finite element results from Ref. 7 and are found to be in good agreement. These results validate the present finite element model, COMPZ.

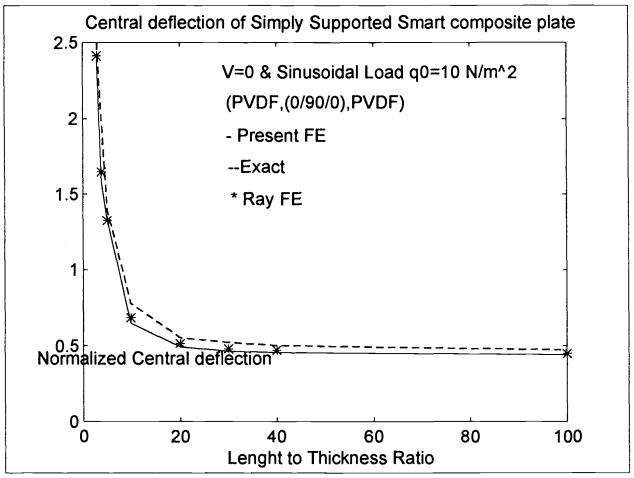

Figure 5. Center Deflection vs. Length to Thickness ratio for a Plate Subjected to a Double Sinusoidal Mechanical Load

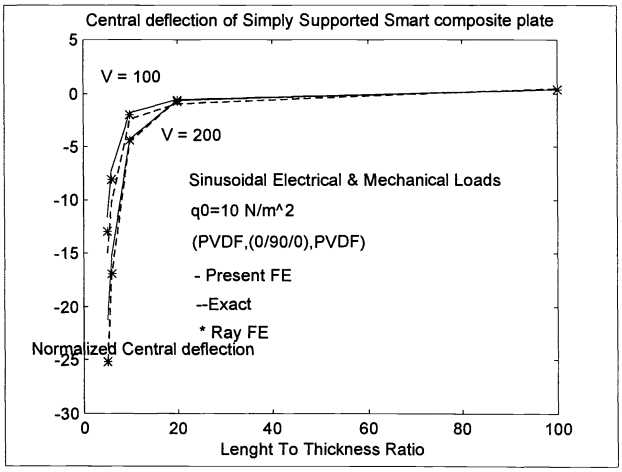

Figure 6. Center Deflection vs. Length to Thickness ratio for a Plate Subjected to Double Sinusoidal Electrical and Mechanical Loads

To demonstrate the use of OPTSHP to determine optimum actuator voltages, a square 0.45m X 0.45m plate with three layers ($0^0/90^0/0^0$) is used and piezoelectric actuators are placed on the top surface. The length to thickness ratio equals to fifty. The plate is divided into nine elements, as shown in Fig. 7. The properties of the graphite/epoxy and piezoelectric actuators are the same as in the previous example.

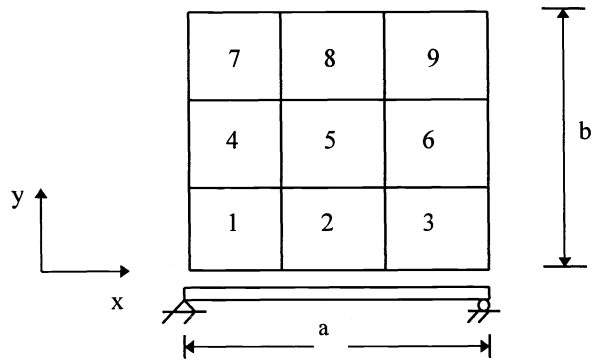

Figure 7. Finite Element Model of Composite Plate with Piezoelectric Actuator

The original shape is chosen as a flat plate (z_0) and the desired shape is selected as

$$z_{des} = 1 \times 10^{-9} x^2 - 4.2 \times 10^{-10} xy + 6 \times 10\text{-}8\, y^2 \tag{35}$$

Table 1 gives the optimum voltages and error function when two actuators are used. Table 2 gives the optimum voltages and error function when four actuators are used. In both cases, the optimization program f-mins is used to determine optimum actuator voltages and voltages are unconstrained. The results show that the locations of the actuators have significant influence on the optimum voltages and the error function.

Table 1. Optimal Actuator Voltages and Error Functions for the Case of Use of Pair of Actuators

Actuators Positions	Minimum Applied Voltages (Volt.)	*Minimum Error Function*
Elements #s 1 & 7	$V_1 = 41.612$ $V_7 = 47.265$	f= 5.78007896e-18
Elements #s 2 & 8	$V_2 = 35.943$ $V_8 = 39.934$	f = 4.74678213e-18
Elements #s 3 & 9	$V_3 = 85.710$ $V_9 = 90.547$	f = 4.0583368e-18
Elements #s 1 & 3	$V_1 = -26.368$ $V_3 = 175.055$	f = 4.10114654e-18
Elements #s 4 & 6	$V_4 = -8.231$ $V_6 = 79.660$	f = 4.01544062e-18
Elements #s 7 & 9	$V_7 = 26.0895$ $V_9 = 175.193$	f = 4.09288468e-18
Elements #s 1 & 9	$V_1 = -17.007$ $V_9 = 170.053$	f = 4.10970645e-18
Elements #s 3 & 7	$V_3 = 169.712$ $V_7 = -16.138$	f = 4.12087738e-18

Table 2. Optimal Actuator Voltages and Error Functions for the Case of Use of Four Actuators

Actuators Positions	Minimum Applied Voltages (Volt.)	*Minimum Error Function*
Elements #s 1, 3, 7 & 9	$V_1 = -21.060$ $V_3 = 98.104$ $V_7 = -16.473$ $V_9 = 101.482$	f = 4.0531138e-18
Elements #s 2, 4, 8 & 6	$V_2 = 18.404$ $V_4 = -29.429$ $V_6 = 65.262$ $V_8 = 22.349$	f = 4.01531283e-18

6. CONCLUSIONS

A finite element model was developed for composite plates with pizoelectric actuators and sensors. The plate was composed of distributed sensors and actuators made of PVDF or PZT and a laminate of graphite/epoxy layers. A simple higher-order deformation theory was used. A Hermite cubic interpolation function was used to approximate the transverse deflections. This method does not suffer from shear correction which is problematic in the first-order shear deformation theory. The displacement model includes the parabolic distribution of the transverse shear stresses and the non-linearity of in-plane displacement across the thickness. Seven degrees of freedom were used at each node. The number of degrees of freedom used in the present model is one third the number of degree of freedom of the element used in the model developed based on higher-order shear deformation theory. The electric potential was treated as a generalized electric coordinate like generalized displacement coordinate. A Matlab code 'CMPZ' was developed using this approach. The numerical results generated by the developed code agree very well with the analytical solution and other published finite element results.

For shape control, an objective error function was formulated which is a summation of the mean square error between a point in the actual surface and a corresponding point in the desired surface integrated over the element surface. This approach is an improvement over the method where surface error is determined only at the nodal pints. Matlab optimization functions f-min and f-mins were used to determine optimum actuator voltages in order to minimize objective error function. A Matlab code 'OPTSHP' was developed using this approach for shape control. The numerical results demonstrate the feasibility of using piezoceramic actuators for correcting antenna surface errors.

7. REFERENCES

1. E. F. Crawley, "Intelligent structures for aerospace: A technology overview and assessment", AIAA J., Vol. 32, No. 8, 1994.
2. J. N. Reddy, "A simple higher order theory for laminated composite plates", J. Appl. Mech., pp 745-752, 1984.
3. K. Ghosh and R. C. Batra, "Shape control of plates using piezoceramic elements", AIAA J., 1995
4. S. K. Agrawal and D. Tong, "Modeling and shape control of piezoelectric actuator embedded elastic plates", J. Int. Material Sys & struct., Vol. 5, July 1994.
5. D. B. Koconis, L. P. Kollar and G. S. Spinger, "Shape control of composite plates and shells with embedded actuators: I. Voltage specified, II. Desired shape specified", J. Composite Materials, Vol. 28, No. 5, pp 415-483, 1994.
6. M. C. Ray, R. Bhattacharya, and B. Samanta, "Exact solution for static analysis of intelligent structures", AIAA J., Vol. 31, No. 9, September 1993.
7. M. C. Ray, R. Bhattacharya and B. Samanta, "Static Analysis of an intelligent structure by the finite element method", Computer & Structures, Vol. 52, No. 4, pp 617-613, 1994.